RESEARCH ARTICLE

Macromolecular Rapid Communications
www.mrc-journal.de

Preparation and Characterization of Novel Poly(thiourethane)–Poly(isocyanurate) Covalent Adaptable Networks: Effect of the Catalysts

Federico Guerrero, Silvia De la Flor, and Àngels Serra**

Poly(thiourethane)-based covalent adaptable networks are synthesized by reacting a trimer of hexamethylene diisocyanate (Desmodur N3300) containing isocyanurate groups in its structure with 1,6-hexanedithiol. The catalysts evaluated for this process include dibutyltin dilaurate (DBTDL), lanthanum triflate ($La(OTf)_3$), and a thermal precursor of 1,8-diazabicyclo[5.4.0]undec-7-ene (BGDBU). The use of DBTDL results in the initiation of curing upon mixing, while the other two catalysts exhibit a latency period in the reactive mixture, with curing starting at about 90 °C. Notably, the use of the lanthanum salt produces an additional minor exothermic reaction at 80 °C. This phenomenon corresponds to the trimerization of isocyanates rending isocyanurates, leaving a portion of unreacted thiols. Materials prepared with BGDBU or $La(OTf)_3$ present shorter relaxation times than those prepared with DBTDL. Nevertheless, the materials containing the lanthanum salt do not reach complete relaxation, likely due to the reinforcement of the permanent network through increased isocyanurate content. The formation of isocyanurates produces a stoichiometric imbalance, leaving unreacted thiols. This transforms the exchange process into a dual mechanism involving a dissociative process of thiourethanes to isocyanate and thiol, along with an interchange through thiol attacking the thiourethane group. The materials exhibit good recyclability and self-healing characteristics.

1. Introduction

For about a hundred years, polymeric materials have played a priority role in the development of our society. However, in the last decade, we are conscious of the environmental problem that starts when their service life is over. Plastics are being found everywhere in nature, many in the seas, and this pollution is an environmental problem and a significant health threat.

Thermoplastics can be recycled with adequate waste management, but thermosetting polymers cannot, and finally, there are incinerated or landfilled.[1] Due to this fact, many researchers are making great efforts to solve this problem. In 1946, Stern and Tobolsky reported an unexpected behavior in some thermosetting polymers which could be reprocessed without losing their properties, as if they were thermoplastics.[2] Nowadays, these materials are named covalent adaptable networks (CANs), an intelligent solution to the problem of the lack of recyclability of thermosets: the presence of reversible groups gives dynamic nature to the material. Covalent bonds in the network structure experiment an exchange reaction that allows recycling, self-healing, and self-welding after a convenient stimulus (temperature or light).[3–6] This exchange reaction can follow a dissociative mechanism (in which the cross-linking density decreases) or an associative mechanism (in which there is no loss of connectivity). CANs that follow this second mechanism were reported by Leibler and co-workers in 2011,[7] and they are called "vitrimers." Different cross-linked polymeric materials have been described as CANs, for example, poly(urethane)s (PUs).

Polyurethanes are one of the most produced polymers in the world (5.5% in 2021)[8] with applications in binders, coatings, elastomers, and flexible and rigid foams. The sulfur analogs of poly(urethane)s are the poly(thiourethane)s ((PTU)s). Despite some advantages that are present in reference to the oxygenated analogs, such as excellent optical properties and better biocompatibility,[9,10] they have not been so widely studied.[11] In our research team, we have studied the preparation of poly(thiourethane) networks with vitrimer-like properties and easy recycling and reshaping,[12–15] and also composites with poly(thiourethane) matrix with good dispersion and enhanced

F. Guerrero, À. Serra
Department of Analytical Chemistry and Organic Chemistry
Universitat Rovira i Virgili
C/ Marcel·lí Domingo s/n Edif. N4, Tarragona 43007, Spain
E-mail: angels.serra@urv.cat
S. De la Flor
Department of Mechanical Engineering
Universitat Rovira i Virgili
Av. Països Catalans, 26, Tarragona 43007, Spain
E-mail: silvia.delaflor@urv.cat

The ORCID identification number(s) for the author(s) of this article can be found under https://doi.org/10.1002/marc.202400330

DOI: 10.1002/marc.202400330

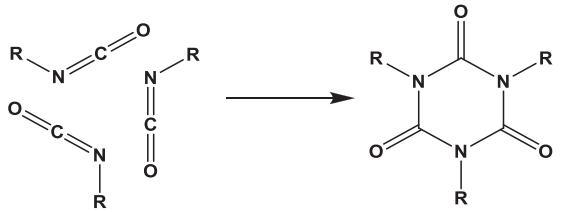

Scheme 1. General reaction of trimerization of isocyanate groups producing an isocyanurate ring.

mechanical and vitrimeric properties.[16] We prepared these materials by a reaction between multifunctional thiols and diisocyanates in the presence of acidic catalyst such as dibutyltin dilaurate (DBTDL)[12,13] or lanthanide triflates ($Ln(OTf)_3$),[17] or basic catalysts as 1-methylimidazol or 1,8-diazabicyclo(5.4.0)undec-7-ene (DBU), as well as their tetraphenylborate salts.[14]

The most common chemical providers offer a wide catalog of monomers containing thiols with different functionalities and structures. However, the catalog of isocyanate monomers is limited to diisocyanates as hexamethylene diisocyanate (HDI), isophorone diisocyanate, bis(cyclohexyl isocyanate), or isomers of toluene diisocyanate. The most industrially used triisocyanate monomers are derived from trimerization of different diisocyanates and are fabricated by Covestro.[18] These triisocyanates contain isocyanurate rings, one of the most important by-products in PU preparation due to its symmetry and the especially stable ring (**Scheme 1**).[19] For their properties, functionality, and thermodynamic stability, isocyanates containing isocyanurate groups are employed in industry as a hardener in coating systems and biomedical materials, mainly aliphatic, and in flame-retardant material, mainly aromatics. They are a safer alternative to simple isocyanates, which are toxic by inhalation, presenting a higher viscosity that, and in some cases, require the use of a solvent to control the rheological behavior. A wide variety of catalysts have been employed for the preparation of poly(isocyanurate)[20] and poly(urethane-isocyanurate) materials such as tetrabutylammonium fluoride,[21] proazaphosphatrane,[22] N-heterocyclic carbenes (NHCs),[23] tin(IV) compounds,[24] rare-earth metal complexes,[25] potassium methoxide,[26] or palladium(0) systems,[27] as examples.

As far as we know, this is the first publication that reports the use of industrial triisocyanates in the preparation of PTU, and the first preparation and study of poly(thiourethane-isocyanurate) networks. We propose the preparation of PTU materials, using as starting product Desmodur N3300, a commercial trimer of HDI, and 1,6-hexanedithiol. As catalyst, we have tested an organometallic compound of Sn(IV) (DBTDL), a rare-earth metal triflate ($La(OTf)_3$), and an organic base generator (1,8-diazabicyclo[5.4.0] undec-7-ene tetraphenylborate, BGDBU) in different concentrations. The structures of the starting products and catalyst used are depicted in **Scheme 2**. We have determined the effect of each catalyst in the network structure and the thermomechanical characteristics derived, paying special attention to the stress-relaxation ability. From our previous studies, we know the important role of the catalyst and its proportion on the times and temperatures needed to relax the stresses and applications that can be derived from them. Because of the industrial availability of Desmodur N3300 and the final characteristics of the materials obtained, a broad technological application can be foreseen.

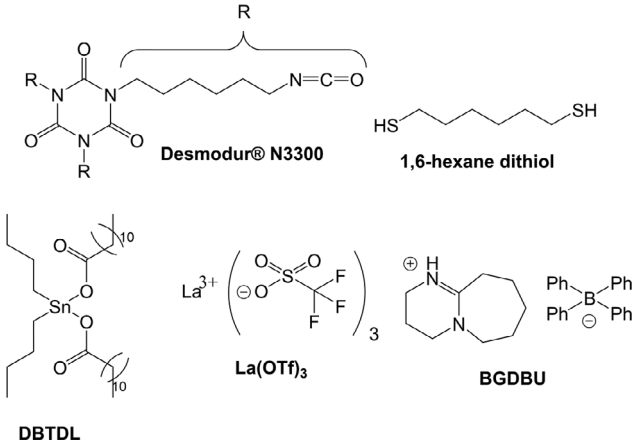

Scheme 2. Structure of the monomers and catalysts.

2. Experimental Section

2.1. Materials

Desmodur N3300 was kindly supplied by Covestro. 1,6-hexane dithiol and chlorotrimetylsilane were from Thermo Scientific. DBTDL was from Merck. $La(OTf)_3$ was from Aldrich. Acetone and chloroform were from Scharlab. 1,2-dichlorobenzene was from Panreac. All products were used as received, except acetone, which was dried following standard procedures. BGDBU was synthesized from DBU and sodium tetraphenyl borate according to a reported methodology.[28] The structure of monomers and catalysts are shown in Scheme 2.

2.2. Preparation of the Formulations

Thiol (1,6-hexaneditiol) and triisocyanate (Desmodur N3300) were mixed in stoichiometric proportions: 1 mol of thiol group per mol of isocyanate group. The amount of catalyst was calculated as mols of catalysts per hundred mols of theoretical thiourethane groups. The composition of formulations is shown in **Table 1**.

Samples with lanthanum triflate and organic salt required dry acetone to solve the crystalline catalysts. Once solved in the minimum amount, acetone was eliminated under reduced pressure

Table 1. Composition of the formulations.

	Isocyanate [g]	Thiol [g]	Catalyst [mg]
DBTDL 0.5%	3	1.16	48.7
DBTDL 1%	3	1.16	97.4
$La(OTf)_3$ 0.5%	3	1.16	45.2
$La(OTf)_3$ 1%	3	1.16	90.4
BGDBU 0.25%	3	1.16	19.2
BGDBU 0.5%	3	1.16	38.4

at room temperature. The proportion of BGDBU used was 0.5% and 0.25% in mol due to the lower solubility of this catalyst in the mixture.

2.3. Preparation of Materials

The materials were prepared using a Petri dish previously silanized with a solution of chlorotrimethyl silane in chloroform (10% in volume). The formulations were spread on the surface and placed in an oven at 90, 100, 110, and 120 °C (for 30 min each temperature), 140 °C (for 1 h), and 160 °C (for 2 h). After curing, samples were demolded while still hot.

2.4. Calorimetric Study

A differential scanning calorimeter (DSC) Mettler DSC-3+ was calibrated using an indium standard (heat flow calibration), and an indium–lead–zinc standard (temperature calibration) was used to analyze the curing evolution.

Mixture quantities of ≈10 mg were tested in aluminum pans with a pierced lid in an inert atmosphere (N_2) with a gas flow of 50 cm^3 min^{-1}. The dynamic studies were performed in a temperature range of 0–200 °C with a heating rate of 10 °C min^{-1}. The glass-transition temperatures (T_gs) of the cured materials were determined by heating a small piece of cured material between 0 and 200 °C at 25 °C min^{-1}. Enthalpies and glass transition temperatures were calculated with the help of the STARe software.

2.5. Thermal Stability

The thermal stability of the cured samples was evaluated by thermogravimetric analysis (TGA) using a Mettler Toledo TGA2 thermobalance. All experiments were performed under an inert atmosphere (N_2 at a flow of 50 cm^3 min^{-1}). Pieces of 20–30 mg of cured samples were degraded between 30 and 800 °C, with a heating rate of 25 °C min^{-1}.

2.6. Infrared Spectra

Fourier-transform infrared (FTIR) spectra were recorded with a spectrometer Jasco FTIR 6700, in absorbance mode, with a resolution of 4 cm^{-1}, in the wavelength range from 400 to 4000 cm^{-1}, and with 32 scans of each spectrum.

2.7. Raman Spectroscopy

Raman spectra were recorded with a spectrometer Raman Renishaw InVia, with a resolution of 1 cm^{-1} in the spectral range from 400 to 3100 cm^{-1}.

2.8. Viscoelastic and Thermomechanical Properties

The viscoelastic and thermomechanical properties were evaluated using a thermal dynamic mechanical analyzer (DMA) Q800 analyzed from TA Instruments using a film tension clamp. Cured samples were die-cut in about 20 mm × 5 mm rectangular areas.

The evolution of tanδ and storage modulus with the temperature was investigated at a heating rate of 3 °C min^{-1} from −50 to 200 °C, at 1 Hz and 0.1% strain.

Tensile-stress-relaxation tests were conducted using samples with the dimensions previously defined. The samples were equilibrated at 155 °C and left at this temperature for 5 min. Then, a constant strain of 1.5% was applied (to ensure the materials were within the linear range), and the consequent stress level was measured as a function of time for 2 h. Then, the temperature was increased 5 °C, and the process was repeated until the final temperature of 180 °C was reached. Relaxation stress $\sigma(t)$ was normalized to the initial stress (σ_0), and the relaxation time (τ) was determined as the time necessary to relax $0.37\sigma_0$. With the relaxation times obtained at each temperature, the activation energy values (E_a) and the pre-exponential factor (A) were calculated by using an Arrhenius-type equation

$$\ln(\tau) = \frac{E_a}{RT} - \ln(A) \quad (1)$$

where τ is the time needed to attain a given stress-relaxation value ($0.37\sigma_0$), R is the gas constant, and T the absolute temperature. The topology freezing temperature (T_v), the temperature at which the material reaches a viscosity of 10^{12} Pa s, was obtained from the Arrhenius equation. Using Maxwell's relation and E' determined from DMA (assuming E' was relatively invariant in the rubbery state), τ^* was determined for each sample. The Arrhenius relationship was then extrapolated to the corresponding value of τ^* to determine T_v for each sample.

To determine the viscosity at each temperature needed to represent the Angell fragility plot, a series of creep experiments were performed on films, taking temperatures between 140 and 190 °C, with an increase of 5 °C in each test. To perform the essays, the selected temperature was maintained for 3 min, and a stress level of 0.1 MPa was applied for 30 min. The viscosity η (Pa s) was obtained from the creep curves, considering the linear part of the variation of the strain and fitting it with linear regression. The strain rate $\dot{\epsilon}$ was obtained from the slope of the linear fit. The viscosity η was calculated according to the following equation

$$\eta = \frac{\sigma}{\dot{\epsilon}} \quad (2)$$

and represented against T_g/T, obtaining the Angell fragility plot.

2.9. Tensile Tests

Tensile strength tests were performed in dog-bone type V samples at room temperature, using an electromechanical universal testing machine UTS Shimadzu AGS-X with a 1000 N load cell at 5 mm min^{-1} according to American Society for testing and materials (ASTM) D638-14 standard. Three samples of each material were tested, and the average results were presented.

2.10. Recycling

The recycled samples were obtained by cutting the cross-linked polymer into small pieces and hot-pressing at 15 MPa in an

aluminum mold at 190 °C for 30 min. Recycled samples were die-cut in dog-bone shapes from the new film obtained and were tested by DMA (to obtain the thermomechanical properties) and Universal Test Machine (to obtain the tensile strength). By FTIR, the permanence of the chemical structure was confirmed.

2.11. Self-Healing Tests

Self-healing tests were made by scratching the specimens with a doctor's blade. Then, they were maintained in an oven at 190 °C for 30 min and were inspected from time to time to monitor the evolution of the scratch by taking photographs using a Digital Microscope Leica DMS1000.

2.12. Gel Content Determination

The determination of gel content in the materials was conducted as follows: small pieces of the materials weighing 0.1–0.2 g (previously dried under reduced pressure at 80 °C overnight) were initially weighed (m_0) before being introduced into a vial containing 1,2-dichlorobenzene. The vial was closed, heated at 150 °C for 24 h, and then cooled to room temperature. The polymer sample was dried under reduced pressure at 80 °C overnight. Then, the sample was weighed again (m), and the gel content was calculated using Equation (3)

$$\text{Gel content } (\%) = 100\left[1 - \left(\frac{m_0 - m}{m_0}\right)\right] \quad (3)$$

3. Results and Discussion

3.1. Study of the Curing Process

Thiol–isocyanate reactions can be performed with acidic and basic catalysts. The most typical catalyst is a Lewis acid, DBTDL. However, in a recent work of our group, we demonstrated that $Ln(OTf)_3$ also catalyzes the curing process.[17] Moreover, these lanthanide salts lead to a faster stress relaxation than DBTDL of the cross-linked materials prepared. Finally, the toxicity of lanthanide salts is much lower than Sn(IV) complex, being also water and oxygen tolerant.[29,30] Among lanthanide triflates, the lanthanum salt demonstrated the highest efficacy in stress relaxation, prompting its selection for the current study. Previous publications from our research team have outlined the benefits of organic base generators, such as BGDBU, which not only facilitate temporal control of the curing process but also enhance the relaxation rate of vitrimeric materials.[14,31] Taking these precedents into account, we selected these three catalysts and tested them in different proportions to cure the three-functional Desmodur isocyanate with a difunctional thiol, 1,6-hexane dithiol to see the effect of the catalyst in the curing process, in the material's characteristics and relaxation behavior. Stoichiometric formulations of comonomers were used to reach the highest cross-linking degree.

The curing process of the different formulations with 0.5% mol mol^{-1} of catalysts was investigated by DSC. The obtained curves are shown in **Figure 1** and Figure S1 (Supporting Information). The most significant data extracted are collected in **Table 2**.

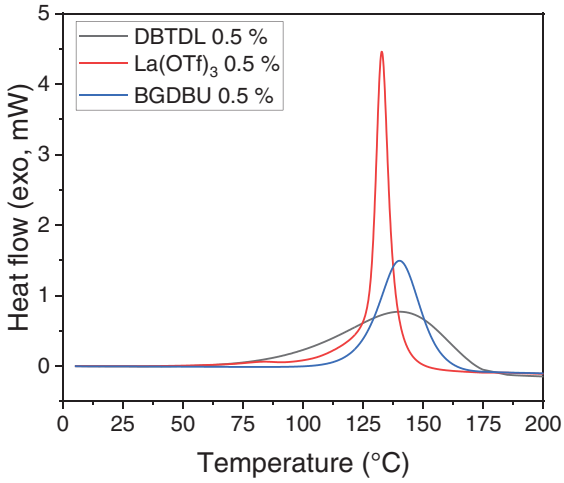

Figure 1. DSC curves for the curing of formulations catalyzed by 0.5% mol mol^{-1} of the different catalysts.

As can be seen, the shape of the curves is quite different. Whereas the formulation containing DBTDL produces a broad exotherm with a relatively undefined starting point, $La(OTf)_3$ sample leads to a very sharp exotherm, which indicates that when the reaction starts, the curing rate is very fast, even faster than the curing using the organic base generator, BGDBU. This can explain what happened during the preparation of the formulation. The addition of DBTDL slowly started the curing, even at room temperature, and the increase in the mixture's viscosity could be noticed, compromising the stability of the formulation. By contrast, the other two formulations did not increase the viscosity overnight. When we increased the amount of catalyst in the samples with DBTDL, only a small shift of the curve at lower temperatures could be observed (Figure S1a, Supporting Information). However, no differences could be observed in the mixture with BGDBU (Figure S1b, Supporting Information) when the amount of catalyst was reduced. This is because DBU, the real catalyst, is not released until reaching a temperature of 90 °C. Thus, this catalyst can be considered a latent catalyst that becomes only active at high temperatures, as was described previously.[13] In the samples catalyzed by $La(OTf)_3$, we could realize that on in-

Table 2. Main calorimetric data extracted from DSC studies for the curing of the formulations studied.

Sample	T_{max} [a] [°C]	ΔH [b] [kJ eq^{-1}]	T_g [c] [°C]
DBTDL 0.5%	141	76	62
DBTDL 1%	127	79	60
$La(OTf)_3$ 0.5%	137	68	62
$La(OTf)_3$ 1%	130	50	45
BGDBU 0.25%	141	57	62
BGDBU 0.5%	141	62	61

[a] Temperature of the maximum of the exotherm; [b] Enthalpy released in the thiol–isocyanate reaction by equivalent of isocyanate; [c] Glass transition temperature of the cured material.

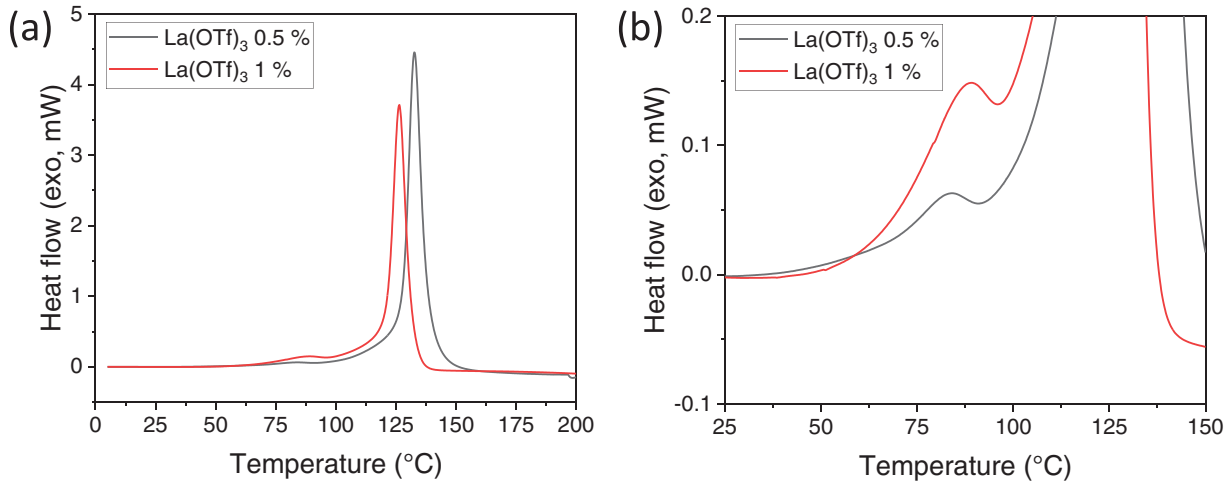

Figure 2. a) Calorimetric curves and b) enlargement of the curing of the formulations with 0.5% and 1% mol mol^{-1} of La(OTf)$_3$.

creasing its proportion in the formulation, there is an increase in the intensity of a small peak at about 80 °C and the shift of the main exotherm at lower temperatures, as can be observed in **Figure 2**. In a previous study on the curing of HDI with trimethylolpropane tris(3-mercaptopropionate (Figure S3, Supporting Information) using different lanthanide triflates as catalysts, we also observed a small peak at similar temperatures, which was attributed to the formation of isocyanurate rings by cycloaddition of isocyanates.[17] The structure of this moiety was confirmed by FTIR analysis. In the published study, the formation of isocyanurates was more evident in the lanthanum salt and less in the ytterbium counterpart. Thus, the size and the coordination ability of the cation affect the formation of this isocyanurate structure.

The data presented in Table 2 show that the curing enthalpies are in the range of 50–80 kJ mol^{-1}, similar to those obtained in other thiol–isocyanate formulations.[31] Any significant effect of the catalyst concentration in the enthalpy is observed, except for La(OTf)$_3$ formulations. In this case, the enthalpy measured corresponds to the second of the two processes observed by DSC: a higher amount of triflate leads to a higher conversion of isocyanate to isocyanurate at 80 °C and, for that, to a lower amount of free isocyanate groups that can react with thiols at a higher temperature and consequently to a lower reaction enthalpy. The T_g remains generally similar in all cases, and it seems not influenced by the catalyst and its proportion. Again, in La(OTf)$_3$ materials, we can observe an exception to this behavior, a significative reduction of glass transition temperature when the amount of triflate increases. It can be explained by the isocyanurate formation that leads to excess free thiols in the final material, changing the structure of the network.

The cured materials were studied by infrared and Raman spectroscopy. FTIR spectra of materials with the same amount of each catalyst are shown in **Figure 3**. FTIR spectra of materials with different amounts of the catalysts studied are presented in Figure S2 (Supporting Information).

In the FTIR spectra, we can observe the total absence of the band in the NCO stretching region (2250 cm^{-1}), confirming that all isocyanate groups have reacted. At 3300 and 1650 cm^{-1}, the N—H and C═O stretching of the thiourethane group can be observed. As reported in a previous paper,[17] C═O stretching of the isocyanurate group absorbed at 1680 cm^{-1} overlapped with the thiourethane absorption. This fact hinders the relative quantification of both groups and the evaluation of the proportion of isocyanurate moieties formed when the lanthanum salt has been used as the catalyst. Due to the presence of isocyanurates in the Desmodur oligomer, few differences in the spectra could be observed among the three catalysts. Thus, FTIR spectroscopy allows us to dismiss the free isocyanate group's presence and confirm that the curing has been completed. However, it does not give much information about the secondary reaction of the isocyanate cyclotrimerization. Moreover, it does not allow us to know the presence or absence of the free thiol group since the S—H stretching (2600–2550 cm^{-1} region) presents a negligible absorbance in this technique. For this reason, we have recorded Raman spectra (**Figure 4**), in which thiol groups present a significative absorption in this region. When we zoom in on this region, we can observe the presence of free thiols in the materials prepared with La(OTf)$_3$ because of the isocyanurate formation that reduces the

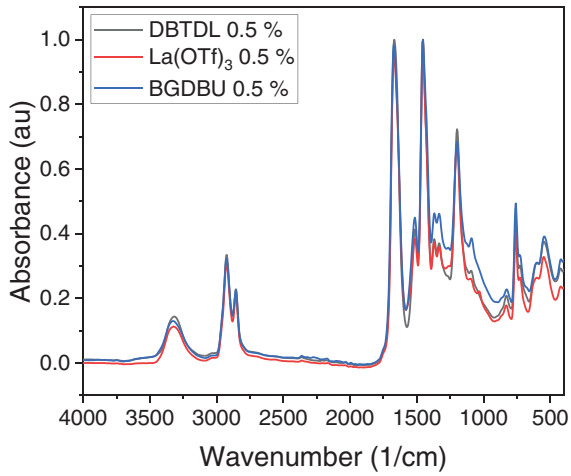

Figure 3. FTIR-attenuated total reflectance (ATR) spectra of the materials prepared with 0.5% of the three catalysts studied.

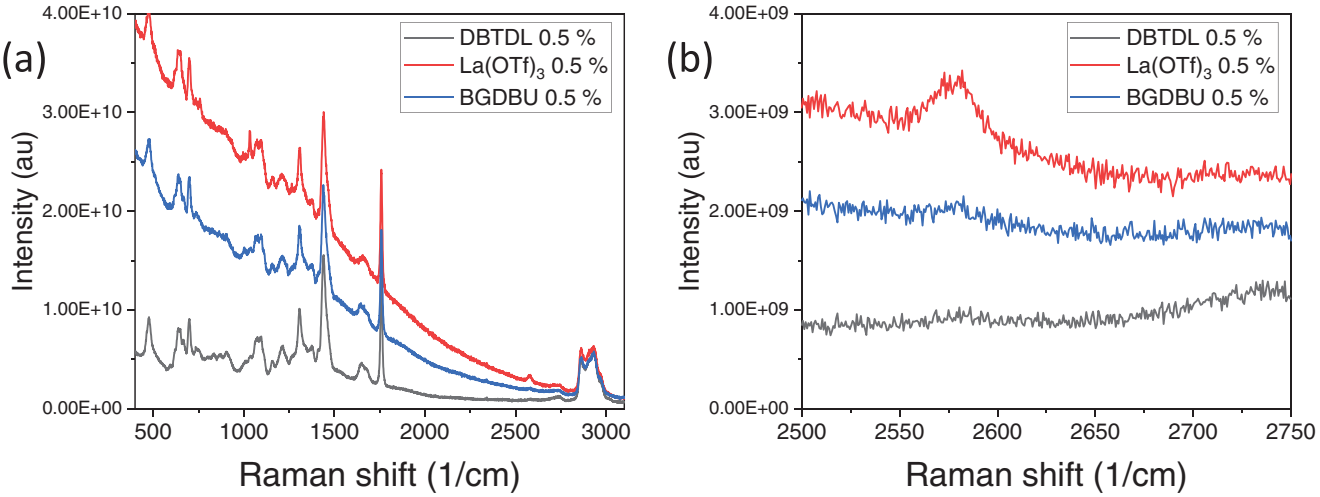

Figure 4. Raman spectra of the materials prepared with a) 0.5% of the different catalysts studied and b) a zoom in 2500–2750 cm^{-1} region.

amount of isocyanate able to react entirely with thiols, confirming indirectly the formation of isocyanurate structures with this catalyst.

Since using $La(OTf)_3$ leads to the loss of stoichiometry in isocyanate/thiol groups, it is valuable to determine the gel content to know if this affects the network integrity. In **Figure 5**, the gel content of these materials, after a dissolution test for 24 h at 150 °C in 1,2-dichlorobenzene, is collected and it is higher than 95% for all the materials except for the materials prepared with this catalyst. The gel content in $La(OTf)_3$ materials diminished by increasing the proportion of catalyst in the formulation. This fact indicates that a small amount of material remains unattached to the network structure, and it solubilizes and also agrees with the lower T_g of these materials.

3.2. Evaluation of the Thermal Stability

The thermal stability of the materials was evaluated by TGA, and the main data extracted are collected in **Table 3**. **Figure 6** shows the first derivative of the weight loss (DTG) of the TGA test of materials with the same amount of each catalyst. DTG curves of the samples prepared with different amounts of each catalyst studied are presented in Figure S3 (Supporting Information).

All materials' initial degradation temperatures are above 200 °C, so they can resist a usual mechanical recycling process,

Table 3. Data obtained from TGA analysis of materials in N_2 atmosphere.

	$T_{2\%}$ [a] [°C]	$T_{5\%}$ [b] [°C]	Char yield [c] [°C]	T_{max} [d] [°C]
DBTDL 0.5%	278	300	5.36	342/470
DBTDL 1%	273	299	6.23	340/469
$La(OTf)_3$ 0.5%	261	290	3.67	336/475
$La(OTf)_3$ 1%	254	286	3.80	328/473
BGDBU 0.25%	260	283	3.49	329/475
BGDBU 0.5%	252	281	3.54	325/471

[a] Temperatures of initial degradation (2% of weight loss); [b] Temperatures of initial degradation (5% of weight loss); [c] Remaining weight percentage at 800 °C; [d] Temperatures of the maximum degradation rates of the two steps.

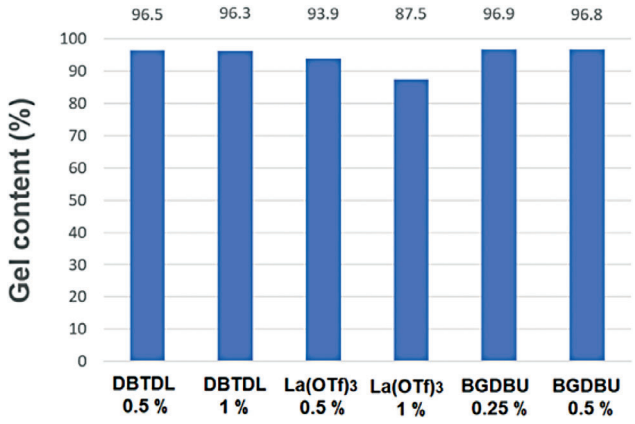

Figure 5. Gel content for all the materials prepared.

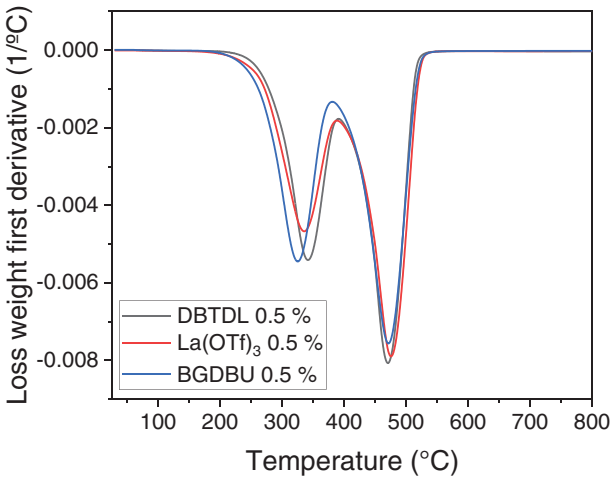

Figure 6. DTG of the curves of the materials prepared with 0.5% of the different catalysts studied in a N_2 atmosphere.

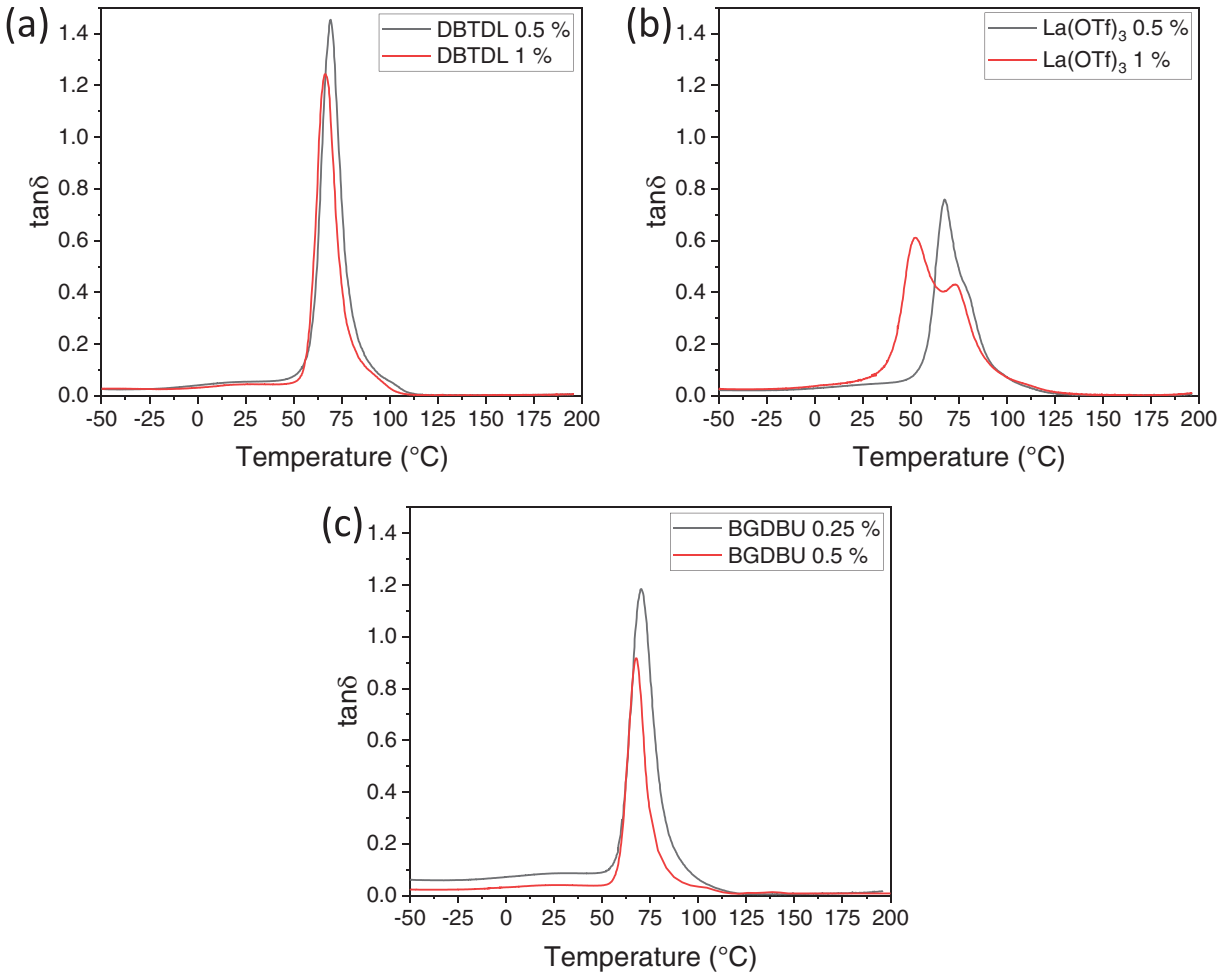

Figure 7. Dependence of tanδ with the temperature of materials prepared with a) DBTDL, b) La(OTf)$_3$, and c) BGDBU as catalysts in different concentrations.

usually performed below 200 °C, without appreciable thermal degradation. In all cases, a higher amount of catalyst leads to an earlier start of the degradation process, because the catalyst also plays a role in these processes. It can also be considered that the presence of some free thiols in La(OTf)$_3$-catalyzed materials could also advance the degradation. At the same catalyst concentration (0.5%), materials prepared using DBTDL present a higher resistance to temperature than those prepared with La(OTf)$_3$ and BGDBU. A later degradation of poly(thiourethane) networks prepared with DBTDL, in comparison with those prepared with lanthanum triflates or base precursors, has been previously reported by our group.[17] The $T_{5\%}$ of a PTU prepared from HDI and S3 was 268 °C using DBTDL and 256 °C using La(OTf)$_3$. In another work of our group, PTU materials prepared from HDI and a mixture (1:3) of thiols derived from limonene and squalene, $T_{5\%}$ was 258 °C with DBTDL and 248 °C with BGDBU.[32] Thus, the initial degradation at lower temperatures when using the lanthanum salt or the DBU salt is a general trend in PTUs. The presence of isocyanurate groups in the Desmodur improves the thermal stability of the cross-linked materials.

The DTG curves of the materials show two main degradation peaks, independently of the catalyst employed. The first step, between 325 and 342 °C, is related to the reversion of thiourethane to isocyanate and thiol.[31] The second, at 469–475 °C, is related to the complete degradation of the network. The reversion of thiourethane groups presents a high dependence on the catalyst employed. With DBTDL, this process occurs at higher temperatures than with La(OTf)$_3$ and BGDBU. However, there is no significant difference when the amount of catalyst is doubled, with the exception of La(OTf)$_3$ materials, which can be explained by the presence of free thiols. The total degradation of the networks does not have any dependence of the catalyst employed and its concentration.

3.3. Thermomechanical Characterization

Materials were characterized by DMA to evaluate their thermomechanical properties and compare them to the same system but using different catalysts and different amounts of catalyst. **Figure 7** shows the evolution of tanδ with temperature. The main data extracted are collected in **Table 4**. Storage modulus evolution with temperature for each material is shown in Figure S4 (Supporting Information).

Table 4. Main data extracted from DMA analysis of several materials prepared.

	$T_{tan\delta}$ [a] [°C]	FWHM [b] [°C]	E_{glassy} [c] [MPa]	$E_{rubbery}$ [d] [MPa]
DBTDL 0.5%	69	12	1552	12.7
DBTDL 1%	67	14	1573	13.1
$La(OTf)_3$ 0.5%	68	24	1669	11.2
$La(OTf)_3$ 1%	52/73	35	1568	8.0
BGDBU 0.25%	70	12	1646	15.2
BGDBU 0.5%	69	18	1631	16.2

[a] Temperature of the maximum of the tanδ peak; [b] Full width at the half height of tanδ peak; [c] Storage modulus obtained at $T_{tan\delta}$ – 50 °C; [d] Storage modulus determined at $T_{tan\delta}$ + 50 °C.

As depicted in Figure 7, variations in the proportion of DBTDL and BGDBU do not significantly affect the thermomechanical properties of materials. Both exhibit similar tanδ curves with a high level of uniformity, although a rise in catalyst quantity marginally enhances heterogeneity (as evidenced by a slight increase in full width at half maximum (FWHM)). However, the ratio of $La(OTf)_3$ notably impacts thermomechanical behavior. The sample $La(OTf)_3$ 0.5% presents a small shoulder at the right side of its tanδ that, when the amount of catalyst is doubled, ends up becoming a well-defined second peak, indicating the presence of a second phase in the network. We could relate this to what was observed in Section 3.1, the existence of a secondary reaction, which consists of forming isocyanurate rings, that breaks the stoichiometric imbalance of the thiol–isocyanate reaction. At the temperature at which the isothermal curing process begins, which is 90 °C, both reactions (trimerization and thiourethane formation) coexist simultaneously. That could generate areas in which trimerization reaction was more favored, giving to the material domains with a higher concentration of isocyanurate and a higher concentration of free thiols. Isocyanurate groups act as a cross-linking point in the structure, so domains in which isocyanurate formation has been more favored would be related to the peak at higher temperature (73 °C). Meanwhile, the peak at 52 °C would be related to the glass transition of the domain in which the thiol–isocyanate reaction has been the most favored.

If isocyanurate rings increase the cross-linking degree, the existence of unreacted thiol groups reduces it. The data of the storage modulus in the rubbery region, strongly related to the cross-linking density, show that the negative effect of free thiols in cross-linking density predominates over the positive effect of the formation of isocyanurate groups, being the storage modulus in this region lower than the obtained in materials prepared with the other two catalysts. On increasing the proportion of the lanthanum catalyst in the formulation, the rubbery modulus also decreases as the result of the lower cross-linking degree.

3.4. Vitrimeric Characterization

Poly(thiourethane) groups, at high temperatures and in the presence of a sufficient amount of an acidic or basic catalyst, can experience an exchange reaction named *trans*-thiocarbamoylation that follows a dissociative mechanism in which the thiourethane group leads to isocyanate and thiol that very fast react to give the thiourethane group again (**Scheme 3a**). Earlier research has demonstrated that this type of material exhibits a vitrimeric-like behavior when heated, as it follows an Arrhenius-type relationship between viscosity and temperature increase.[12–17]

The vitrimeric properties of the prepared materials were evaluated by conducting stress-relaxation experiments using DMA. The chosen temperatures were significantly above the T_g, enabling the structure to exhibit a degree of freedom adequate for the exchange reaction. **Figure 8** illustrates the stress-relaxation curves recorded at 180 °C for materials produced with the maximum quantity of each catalyst, and the key data from all stress-relaxation experiments are summarized in **Table 5**. Figure S5 (Supporting Information) depicts a stress-relaxation experiment at 180 °C for materials prepared with varying amounts of the investigated catalysts.

When comparing samples prepared at the identical catalyst concentration (0.5%), the sample containing BGDBU exhibits the fastest relaxation process, arriving to the characteristic relaxation time in 1.1 min, followed by the $La(OTf)_3$-containing sample in 3 min, and ultimately, the DBTDL sample, achieving a $\sigma/\sigma_0 = 0.37$ in 21.9 min. The accelerated relaxation kinetics of BGDBU samples compared to DBTDL-catalyzed materials has been previously documented in other thiol–isocyanate systems. In the S3/HDI system, Gamardella et al. reported a characteristic relaxation time at 180 °C of 1.3 min with 0.05% BGDBU, while the sample with 0.05% DBTDL did not attain a $\sigma/\sigma_0 = 0.37$ within 1 h.[12] Guerrero et al. observed a similar trend in materials derived from a mixture of thiols from limonene and squalene, and HDI. In the sample with 3:1 limonene/squalene, thiols and 4% BGDBU relaxed $\sigma/\sigma_0 = 0.37$ in 10 s, whereas the equivalent sample with 4% DBTDL took 2.8 min to achieve the same relaxation level.[32]

In contrast to DBTDL, $La(OTf)_3$ demonstrates a faster relaxation process comparable to those determined in BGDBU-catalyzed materials. This observation aligns with findings from a different study involving materials prepared from S3/HDI. In that study, the characteristic relaxation time at 180 °C was 3.5 min for the $La(OTf)_3$ 1% sample and 24 min for the DBTDL 1% sample.[17] The faster exchange kinetics with $La(OTf)_3$ compared to DBTDL could be attributed to the free thiol groups remaining in the material, caused by the trimerization of isocyanate, that can initiate a secondary exchange mechanism, with an attack of the thiol to the electrophilic carbon of the thiourethane group, as shown in Scheme 3b.[33]

Torkelson and co-workers[33] described a relaxation mechanism in polythiourethane networks involving both associative and dissociative processes. They observed that a modest excess of thiol groups (10 mol%) decreases thiourethane reversion, facilitating exchange reactions between thiol and thiourethane groups. This enhancement results in outstanding recovery during repeated recycling steps. Bowman and co-workers explored the thiourethane exchange mechanism, considering the catalyst as a variable.[34] They validated the dual mechanism previously proposed by Torkelson and co-workers, demonstrating its modifiability based on the catalyst's nature.

A noteworthy distinction observed in the stress-relaxation curves is the complete relaxation achieved by the DBTDL and BGDBU materials at 15 and 30 min, respectively. By contrast, the $La(OTf)_3$ sample maintains a consistent residual stress of 4%.

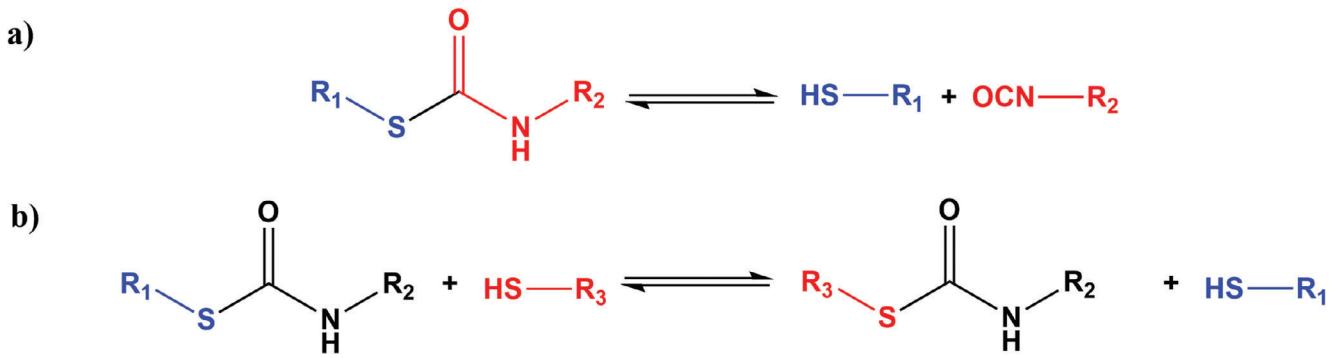

Scheme 3. Possible exchange mechanisms of thiourethane groups in excess thiol. a) Thermal reversion and b) thiol–thiourethane exchange.

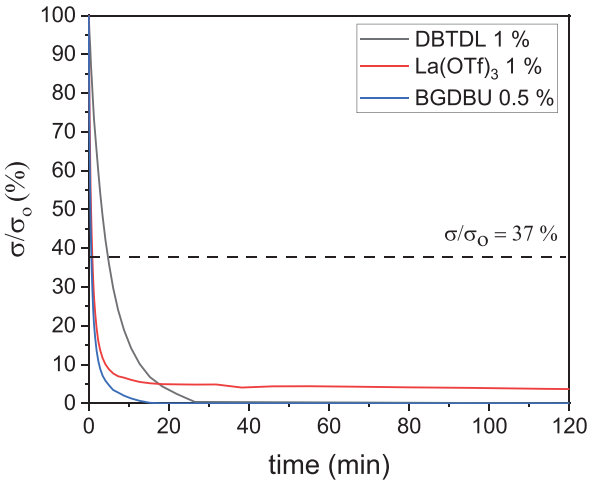

Figure 8. Normalized stress-relaxation curves at 180 °C for materials prepared with the maximum proportion of the different catalysts studied.

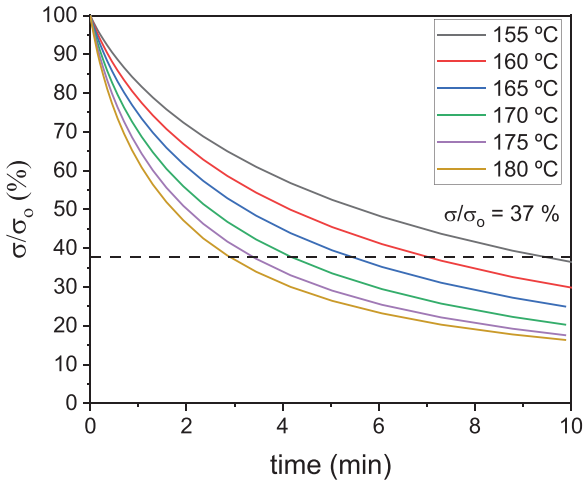

Figure 9. Normalized stress-relaxation curves at different temperatures for the sample La(OTf)$_3$ 0.5%.

This phenomenon may be attributed to the formation of isocyanurate structures that reinforce the permanent network. However, this remaining stress does not impede the reformation of these materials.

To calculate the kinetic parameters of the stress-relaxation phenomena with all catalysts, we conducted stress-relaxation experiments at various temperatures for each material type. **Figure 9** highlights a clear relationship between relaxation time and temperature, with the lanthanum-catalyzed sample serving as a representative illustration.

From the values of $\tau_{0.37}$ at each temperature, the Arrhenius relationships were derived for all the materials. **Figure 10** shows the

Table 5. Main data extracted from stress-relaxation experiments.

	$\tau_{180\,°C}$ [a] [min]	E_a [b] [kJ mol^{-1}]	ln$A$	r^2	T_v [c] [°C]
DBTDL 0.5%	21.9	92	17.2	0.9957	114
DBTDL 1%	8.9	72	12.8	0.9956	85
La(OTf)$_3$ 0.5%	3.0	108	23.6	0.9990	98
La(OTf)$_3$ 1%	1.4	80	16.8	0.9936	68
BGDBU 0.25%	3.4	99	20.8	0.9947	96
BGDBU 0.5%	1.1	77	16.2	0.9953	62

[a] Time to reach a value of $\sigma/\sigma_0 = 0.37\sigma_0$ at 180 °C; [b] Activation energy of the exchange process determined by relaxation of stresses; [c] Topology freezing temperature derived from Arrhenius relationship.

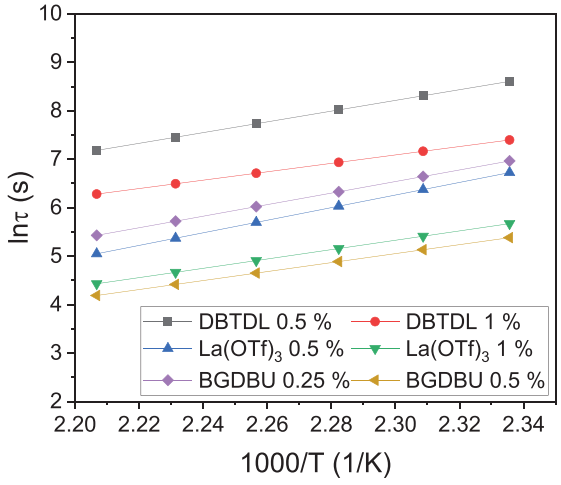

Figure 10. Arrhenius plot of relaxation times against the inverse temperature for all the materials prepared, obtained from relaxation experiments.

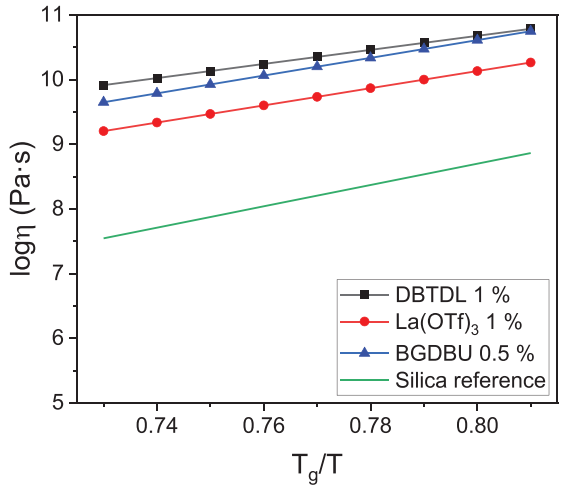

Figure 11. Angell fragility plot of the logarithm of the viscosity as a function of the inverse of temperature. The relation for silica has been included as the reference.

evolution of these values against the inverse of the temperature. The calculated activation energies and the adjusting parameters are included in Table 5.

The plots of relaxation times against inverse temperature fit perfectly with an Arrhenius-type relationship, indicated by the excellent correlation factor, and confirming the vitrimer-like behavior previously reported for poly(thiourethane) networks for all the catalysts tested. The activation energies obtained from the slope of the linear fitting are 72–108 kJ mol^{-1}, reducing in all the cases with the increasing amount of catalyst. From the Arrhenius relationships and using Maxwell equation, we can also determine the T_v, defined as the temperature at which the material reaches a viscosity of 10^{12} Pa s. The calculated T_vs are above $T_{tan\delta}$ in all cases and decrease with the reduction of the catalyst concentration (see Table 5).

After the stress-relaxation tests at different temperatures, in which the materials have been subjected to high temperatures for a long time, the possibility of a structural change or even a degradation of the materials could be possible. By DMA, a second tanδ evaluation was conducted on the relaxed samples without observing any significative change in its tanδ peak, dismissing any structural change or degradation (see Figure S6 in the Supporting Information).

Creep experiments were conducted at various temperatures to derive the Angell fragility plot for the samples containing the higher concentration of each catalyst. The Angell fragility plot is depicted in **Figure 11**. As can be seen, all materials prepared show a linear dependence of the viscosity with relative temperature, similar to vitreous silica and above this reference. Therefore, they can be considered as strong-glass formers, thanks to their vitrimeric character, in contrast to thermoplastics, which are fragile liquids.

Through creep experiments, we determined the activation energies for the three tested materials and, again, their respective T_vs. The activation energies were calculated as 71, 82, and 89 kJ mol^{-1} for the samples containing DBTDL 1%, La(OTf)$_3$ 1%, and BGDBU 0.5%, respectively, very similar to those obtained through stress-relaxation tests. Furthermore, the T_v values derived from creep experiments were somewhat different from the ones obtained through the alternative methodology, measuring 85, 50, and 94 °C for the samples DBTDL 1%, La(OTf)$_3$ 1%, and BGDBU 0.5%, respectively. These differences may be attributed mainly to statistical reasons.

3.5. Recycling

Accordingly, to Figure 10, the material exhibiting the faster relaxation kinetics, namely BGDBU 0.5%, was chosen to validate the recyclability of these materials. The material was cut into small pieces and subjected to hot-pressing at 15 MPa and 190 °C for 30 min. A thermomechanical analysis by DMA was conducted on both the initial BGDBU 0.5% and its recycled counterpart, as depicted in **Figure 12**. The results indicate that the network structure remains unaltered after the recycling process, aligning with our expectations.

A tensile test was conducted on both the pristine and recycled BGDBU 0.5% to assess their stress–strain behavior. For this purpose, samples were die-cut into dog-bone shapes and tested using the UTS Shimadzu AGS-X. Ten samples were tested and the

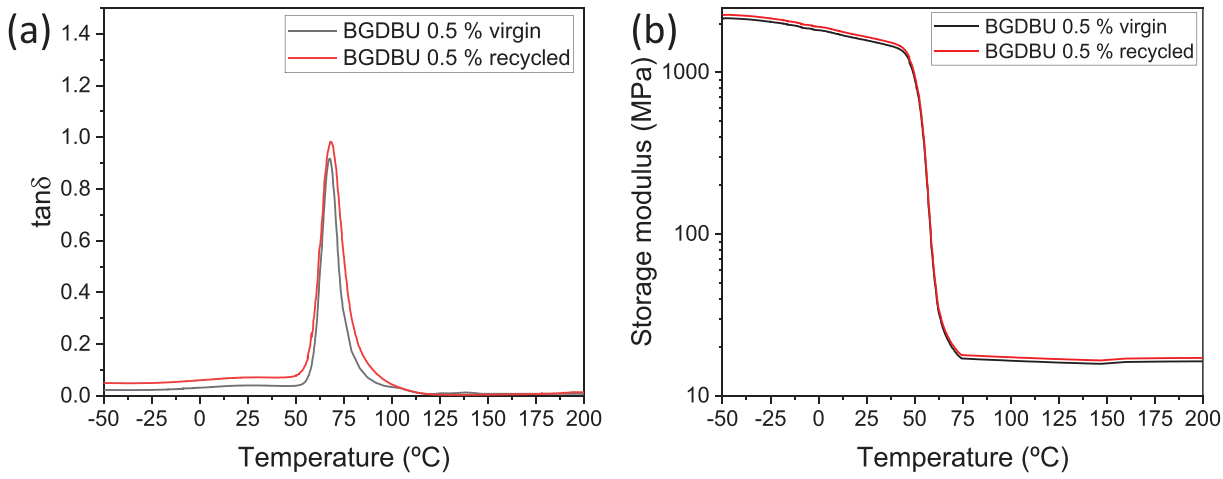

Figure 12. a) Plots of tanδ and b) storage moduli evolution with temperature of the virgin BGDBU 0.5% and after the recycling process.

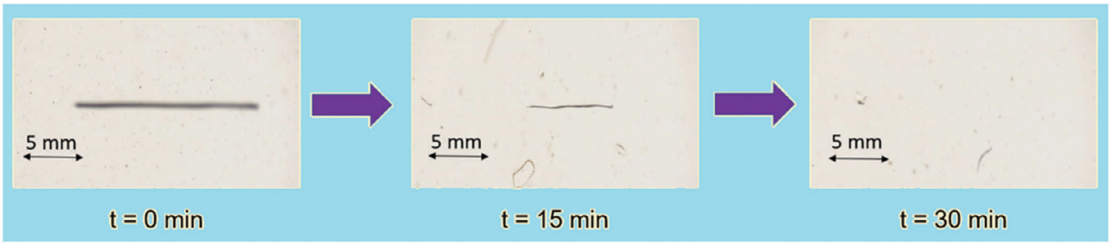

Figure 13. Optical microscope images of the thermal self-healing process at 190 °C at different times for the sample BGDBU 0.5%.

Table 6. Main data extracted from tensile test at break for virgin and recycled sample.

Sample	Stress at break [MPa]	Strain at break [%]	Tensile modulus [MPa]
BGDBU 0.5% virgin	17.6 ± 1.8	1.74 ± 0.2	1360 ± 31
BGDBU 0.5% recycled	15.5 ± 2.3	1.31 ± 0.2	1147 ± 37

average results are summarized in **Table 6**, and a representative stress–strain curve of both materials is plotted in Figure S7 (Supporting Information).

As evident from the mechanical parameters derived from the tensile tests in Table 6, the BGDBU 0.5% sample presents quite similar behavior before and after the recycling process. Minor variations in mechanical properties can be attributed to the exceptionally rigorous conditions of the process and the statistical dispersion of the results. It should be commented that the recycling process was not optimized in time, temperature, and pressure and therefore, these differences in mechanical characteristics can be even reduced.

3.6. Self-Healing Behavior

Self-healing tests were conducted by merely scratching the specimens using a doctor's blade and inspecting the evolution of the scratch at different times through optical microscopy. **Figure 13** presents the optical microscope image illustrating the self-healing process of the BGDBU 0.5% material, which was completed within just 30 min at 190 °C.

The capacity of these materials to self-heal can be attributed to two distinct reversible interactions: the *trans*-thiocarbamoylation reaction between thiourethane groups and the establishment of hydrogen bonding among these groups, working cooperatively. The self-healing process is triggered by temperature, particularly when elevated above the T_g. This dual reorganization mechanism, involving both covalent and noncovalent interactions, was initially proposed by Lehn and co-workers for polymeric iminocarbohydrazides.[35]

4. Conclusions

In this study, novel poly(thiourethane)–poly(isocyanurate) CANs were synthesized and characterized using different catalysts: DBTDL, $La(OTf)_3$, and a thermal precursor of BGDBU. The results showed distinct curing behaviors and efficiencies for each catalyst. DBTDL initiated curing immediately upon mixing, whereas $La(OTf)_3$ and BGDBU exhibited delayed curing, starting around 90 °C. Notably, $La(OTf)_3$ induced an additional exothermic reaction at 80 °C, indicating the formation of isocyanurate rings and a resulting stoichiometric imbalance due to unreacted thiols. Tanδ experiments revealed the presence of domains with varying degrees of cross-linking due to this secondary reaction.

Creep and stress-relaxation experiments confirmed the vitrimer-like behavior of these materials. Materials cured with BGDBU and $La(OTf)_3$ exhibited shorter relaxation times compared to those cured with DBTDL. However, the presence of $La(OTf)_3$ led to an incomplete relaxation, likely due to the reinforcement of the permanent network by the increased isocyanurate content. The dual mechanism of exchange involving both, thermal reversion of thiourethane group and thiol–thiourethane exchange, was evidenced by the resulting material properties.

The materials demonstrated significant recyclability and self-healing characteristics. The BGDBU 0.5% material retained its network structure after mechanical recycling, confirmed by tanδ experiments and tensile test. Self-healing tests indicated that the materials could repair surface damages at elevated temperatures, underscoring their practical potential for applications requiring circularity, durability, and repairability.

These materials represent the first reported poly(thiourethane)–poly(isocyanurate) networks with recyclability and self-healing properties, attributed to the dynamic behavior of the thiourethane group. Additionally, this study is the first to use an industrially available triisocyanate, Desmodur N3300 in PTU preparation, providing a safer alternative to previously employed diisocyanates.

Supporting Information

Supporting Information is available from the Wiley Online Library or from the author.

Acknowledgements

This work was part of the R&D Project No. PID2020-115102RB-C21 funded by Grant No. MICIU/AEI/10.13039/501100011033 and the European Union "NextGenerationEU"/PRTR. The authors acknowledge this grant and also thank to the Generalitat de Catalunya (Grant No. 2021-SGR-00154). The authors also thank Covestro AG for kindly giving them Desmodur N3300.

Conflict of Interest

The authors declare no conflict of interest.

Author Contributions

F.G. conducted the Experimental Section. À.S. wrote the article. S.D.l.F. and À.S. validated the studies, made conceptualization, supervised the work, and reviewed and edited the final paper.

Data Availability Statement

The data that support the findings of this study are available from the corresponding author upon reasonable request.

Keywords

covalent adaptable networks, poly(isocyanurates), poly(thiourethanes), recyclability, self-healing

Received: May 9, 2024
Revised: June 19, 2024
Published online: July 5, 2024

[1] S. Ma, D. C. Webster, *Prog. Polym. Sci.* **2018**, *76*, 65.
[2] M. D. Stern, A. V. Tobolsky, *Rubber Chem. Technol.* **1946**, *19*, 1178.
[3] Y. Jin, Z. Lei, P. Taynton, S. Huang, W. Zhang, *Matter* **2019**, *1*, 1456.
[4] S. J. Garcia, *Eur. Polym. J.* **2014**, *53*, 118.
[5] A. Khan, N. Ahmed, M. Rabnawaz, *Polymers* **2020**, *12*, 2027.
[6] K. Yu, P. Taynton, W. Zhang, M. L. Wunn, H. J. Qi, *RSC Adv.* **2014**, *4*, 10108.
[7] D. Montarnal, M. Capelot, F. Tournilhac, L. Leibler, *Science* **2011**, *334*, 965.
[8] Plastics-the Facts 2022, Plastics Europe, https://plasticseurope.org/knowledge-hub/plastics-the-facts-2022 (accessed: April 2024).
[9] Y. Jia, B. Shi, J. Jin, J. Li, *Polymer* **2019**, *180*, 121746.
[10] B. Jaffrennou, N. Droger, F. Méchin, J. L. Halary, J. P. Pascault, *e-Polym.* **2005**, *5*, 082.
[11] X. Lopez de Pariza, P. Fanlo, L. Polo Fonseca, A. Ruiz de Luzuriaga, H. Sardon, *Prog. Polym. Sci.* **2023**, *145*, 101735.
[12] F. Gamardella, F. Guerrero, S. De la Flor, X. Ramis, A. Serra, *Eur. Polym. J.* **2020**, *122*, 109361.
[13] F. Gamardella, S. De la Flor, X. Ramis, A. Serra, *React. Funct. Polym.* **2020**, *151*, 104574.
[14] F. Gamardella, S. Muñoz, S. De la Flor, X. Ramis, A. Serra, *Polymers* **2020**, *12*, 2913.
[15] F. Guerrero, X. Ramis, S. de la Flor, A. Serra, *React. Funct. Polym.* **2023**, *183*, 105501.
[16] F. Guerrero, S. De la Flor, X. Ramis, J. I. Santos, A. Serra, *Eur. Polym. J.* **2022**, *174*, 111337.
[17] F. Guerrero, F. Gamardella, X. Ramis, S. De la Flor, A. Serra, *Polymer* **2023**, *283*, 126262.
[18] Coatings, paints & inks Adhesives Foams Desmodur: For quality coatings, adhesives and PU foams, https://solutions.covestro.com/en/brands/desmodur (accessed: June 2024).
[19] P. J. Driest, D. J. Dijkstra, D. Stamatialis, D. W. Grijpma, *Macromol. Rapid Commun.* **2019**, *40*, 1800867.
[20] Y. Guo, M. Muuronen, F. Lucas, R. P. Sijbesma, Ž. Tomović, *ChemCatChem* **2023**, *15*, 202201362.
[21] Y. Nambu, T. Endo, *J. Org. Chem.* **1993**, *58*, 1932.
[22] J. N. Gibb, J. M. Goodman, *Org. Biomol. Chem.* **2012**, *11*, 90.
[23] H. A. Duong, M. J. Cross, J. Louie, *Org. Lett.* **2004**, *6*, 4679.
[24] S. R. Sandler, *J. Appl. Polym. Sci.* **1967**, *11*, 811.
[25] T. A. C. Flipsen, R. Steendam, A. J. Pennings, G. Hadziioannou, *Adv. Mater.* **1996**, *8*, 45.
[26] R. J. Arnold, J. A. Nelson, J. J. Verbanc, *Chem. Rev.* **1957**, *57*, 47.
[27] F. Paul, S. Moulin, O. Piechaczyk, P. Le Floch, J. A. Osborn, *J. Am. Chem. Soc.* **2007**, *129*, 7294.
[28] T. Rodima, I. Kaljurand, A. Pihl, V. Mäemets, I. Leito, I. A. Koppel, *J. Org. Chem.* **2002**, *67*, 1873.
[29] S. Hirano, K. T. Suzuki, *Environ. Health Perspect.* **1996**, *104*, 85.
[30] S. Kobayashi, *Synlett* **1994**, *1994*, 689.
[31] F. Gamardella, X. Ramis, S. De la Flor, A. Serra, *React. Funct. Polym.* **2019**, *134*, 174.
[32] F. Guerrero, X. Ramis, S. De la Flor, A. Serra, *Polymers* **2023**, *15*, 1583.
[33] L. Li, X. Chen, J. M. Torkelson, *Macromolecules* **2019**, *52*, 8207.
[34] Z. Wen, X. Han, B. D. Fairbanks, K. Yang, C. N. Bowman, *Polymer* **2020**, *202*, 122715.
[35] N. Roy, E. Buhler, J. M. Lehn, *Polym. Int.* **2014**, *63*, 1400.

